International Journal of Dynamics and Control – Accepted manuscript

Acceleration helps in skateboarding at high speeds

Balazs Varszegi · Denes Takacs · Tamas Insperger

Received: 17 Aug 2017 / Accepted: 22 Oct 2017

Abstract The aim of this study is to investigate the dynamics of an accelerating skater–board system modeling downhill motion. The governing mathematical model is a system of time-varying neutral delay-differential equations. Stability analysis is performed based on the frozen-time method, and the results are verified via numerical simulations. It is shown that the varying longitudinal speed may result in loss of stability at high speeds, which explains the unpredictable falling often observed at real downhill skateboarding. The positive effect of large longitudinal acceleration on the stability is also demonstrated.

Keywords Skateboard · Nonholonomic mechanics · Human Balancing · Acceleration · Time-varying system

1 Introduction

Investigation of skateboard dynamics started almost 40 years ago with Hubbard's papers [1,2]. He showed that the difficulty of skateboarding changes with the speed in an intricate way. This is due to the complexity of skateboard models, which have two main features. First, the dynamics of the skateboards is described by nonholonomic mechanics, where the kinematic constraints determine the motion. Second, the control algorithm behind the skater balancing mechanism involves a reaction time delay.

Nonholonomic mechanics are well studied [3] while the human postural sway during standing still is also extensively investigated [4–6]. In simple skateboard models the connection between the skater and the board is assumed to be rigid the control effort of the skater is not modeled [7,8]. More sophisticated models involving the effect of the skater's actions have also been developed recently. In [9], a complex balancing model was considered, while the skater's reaction time delay was neglected. In [10], the skaters balancing actions were modeled by a PD control subjected to a feedback delay.

High speed skateboard maneuvers appear typically on slopes, where the accelerating motion of the board may also have an effect on the stability. Therefore this paper extends the model of [10] by involving the longitudinal acceleration of the board. Steady state investigation of an accelerating board was performed in [8], but the transients and the human control was not investigated.

The effect of the speed on stability is also important in robotic locomotion [11,12] and has strong relevance in vehicle dynamics [13]. The acceleration here usually makes the system explicitly time dependent, which requires more sophisticated mathematical methods to analyze stability. Furthermore, in case of an accelerating motion, the stability properties are of interest only over a finite time period as the skateboard either reaches the desired speed or it stops in case of breaking. Therefore the traditional stability definitions dealing with asymptotic properties at time going to infinity are not appropriate here, but rather finite-time stability should be

B. Varszegi
Department of Applied Mechanics, Budapest University of Technology and Economics and MTA-BME Lendulet Human Balancing Research Group, Budapest, Hungary
E-mail: varszegi@mm.bme.hu

D. Takacs
MTA-BME Research Group on Dynamics of Machines and Vehicles, Budapest, Hungary

T. Insperger
Department of Applied Mechanics, Budapest University of Technology and Economics and MTA-BME Lendulet Human Balancing Research Group, Budapest, Hungary

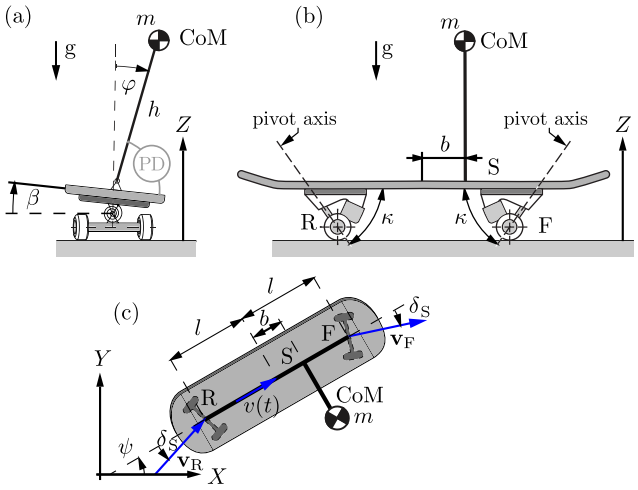

Fig. 1 Mechanical model: front view – panel (a), side view for $\varphi = 0$ and $\beta = 0$ – panel (b) and upper view – panel (c).

investigated. Usually an equilibrium is called stable in finite time sense if the norm of the solution does not exceed a prescribed value. Many other (sometimes even stronger) definitions can be found in the literature, see, e.g., [14,15]. Finite-time stability can alternatively be checked via numerical simulations with given limits for some state variables.

The structure of the paper is as follows. Section 2 presents the derivation of the governing equations for the skater-skateboard model. In Section 3, the linear stability of the investigated rectilinear motion is analyzed via the steady-state and the frozen-time methods and the results are verified by numerical simulations. Section 4 gives explanations on the dynamic loss of stability of skateboarding at high speeds, while section 5 concludes the results.

2 Mechanical, control and mathematical model

The mechanical model under analysis is based on [10], but here a more complex skater-skateboard interaction is considered, which involves both passive and active torques.

2.1 Mechanical model

As it is shown in Fig. 1, the model consists two massless rods, the one between the front (F) and rear (R) points stands for the board, the other one, between the center of mass (CoM) and the ankle joint (S), represents the skater. For the sake of simplicity, we assume, that the ankle joint and the center of rotation of the board around its longitudinal axis are in the same geometrical point, so the two massless rods are connected via a hinge at point S. The following parameters are used: l is the half length of the symmetric board, κ is the angle between the pivot axis and the board in the suspension system, m is the only mass in the system, which stands for the mass of the skater at CoM, h is the distance between the CoM and the ankle joint S, b describes the longitudinal position of the skater on the board, k_t models the torsional stiffness of the board's suspension system and g denotes the gravitational acceleration.

We assume that the board's wheels are in contact with the ground and distance h between the CoM and the ankle joint S is fixed. Thus, the system can be described by five generalized coordinates, which are chosen as follows: x and y describe the position of the board (point S), ψ denotes the direction of the board, while φ and β are the absolute body and board angles around the longitudinal axis of the board respectively.

Due to the skateboards' special suspension system, the axes of the wheels rotates by the steering angle δ_S as the skater tilts the board by the angle β. According to [1], the connection between the steering angle and the orientation of the board is

$$\sin\beta\tan\kappa = \tan\delta_\mathrm{S}. \tag{1}$$

Since perfect rolling is assumed between the wheels and the ground, the directions of the velocities of points F and R are determined uniquely by δ_S and the generalized coordinates, which implies the kinematic constraining equations

$$\begin{aligned}&(\cos\psi\sin\beta\cot\kappa - \sin\psi)\,\dot{x}\\ &+(\sin\psi\sin\beta\cot\kappa + \cos\psi)\,\dot{y} + (l-b)\,\dot{\psi} = 0\,,\end{aligned} \tag{2}$$

$$\begin{aligned}&(\cos\psi\sin\beta\cot\kappa + \sin\psi)\,\dot{x}\\ &+(\sin\psi\sin\beta\cot\kappa - \cos\psi)\,\dot{y} + (l+b)\,\dot{\psi} = 0\,.\end{aligned} \tag{3}$$

In this model, we assume that, the skateboard moves on the horizontal ground and the effect of the slope is taken into account as a third kinematic constraint, which prescribes the longitudinal speed of the board:

$$\dot{x}\cos\psi + \dot{y}\cos\psi = v(t) := at + v_0\,, \tag{4}$$

where v_0 is the initial speed and a is the uniform acceleration caused by the slope.

2.2 Balancing mechanism

The human balancing effort to maintain upright position is modeled via a corrective ankle torque applied at point S between the skater body (S–CoM rod) and the board (F–R rod). This torque can be decomposed into a passive and an active component as

$$M_\mathrm{h}(t) := \underbrace{k\,(\varphi(t) - \beta(t))}_{=M_\mathrm{passive}} + \underbrace{p\varphi(t-\tau) + d\dot{\varphi}(t-\tau)}_{=M_\mathrm{active}}\,, \tag{5}$$

where the muscle stiffness k belongs to the passive torque related to muscle stretching [16], and the active component is modeled as a delayed PD feedback with control gains p and d and reaction delay τ.

2.3 Mathematical model

As the free motion is obstructed by kinematic constraints, the equations of motion can be given using the Kane equations [17], the Gibbs-Appell equations [18] or the extension of the Lagrange-d'Alembert equations [3]. Here, the second one, the Appellian approach is used, which provides the equations of motion in the form

$$\frac{\partial \mathcal{S}(t)}{\partial \dot{\sigma}_i(t)} = \Gamma_i(t)\,, \tag{6}$$

where the acceleration energy $\mathcal{S}$ differentiated with respect to the pseudo accelerations $\dot{\sigma}_i$ equals with the pseudo force Γ_i.

One can chose two pseudo velocities describing the generalized velocities uniquely together with the three kinematic constraints given by Eqs. (2), (3) and (4). Based on [10], we use the pseudo velocities

$$\sigma_1(t) := \dot{\varphi}(t) \quad \text{and} \quad \sigma_2(t) := \dot{\beta}(t)\,, \tag{7}$$

the angular speed of the skater and the board around the longitudinal axis of the board, respectively. The generalized velocities are

$$\begin{bmatrix} \dot{x} \\ \dot{y} \\ \dot{\psi} \\ \dot{\varphi} \\ \dot{\beta} \end{bmatrix} = \begin{bmatrix} v(t)\left(\cos\psi + \frac{b}{l}\tan\kappa\sin\beta\sin\psi\right) \\ v(t)\left(\sin\psi - \frac{b}{l}\tan\kappa\sin\beta\cos\psi\right) \\ -\frac{v(t)}{l}\tan\kappa\sin\beta \\ \sigma_1 \\ \sigma_2 \end{bmatrix}. \tag{8}$$

The acceleration energy of the material point C is

$$\mathcal{S}(t) := \frac{1}{2} m\, a_{\mathrm{CoM}}^2(t)\,, \tag{9}$$

which gives

$$\begin{aligned} \frac{\mathcal{S}(t)}{mh^2} = \Bigg(\left(\sigma_2(t)\cos(\beta(t)) + \frac{\dot{V}(t)}{V(t)}\sin(\beta(t))\right) B\frac{V(t)}{\omega_\mathrm{h}}\cos(\varphi(t)) \\ + \left(1 - H\sin(\varphi(t))\sin(\beta(t))\right) HV^2(t)\sin(\beta(t))\cos(\varphi(t))\Bigg) \\ \times \omega_\mathrm{h}^2\dot{\sigma}_1(t) + \frac{1}{2}\dot{\sigma}_1^2(t) + \dots\,, \end{aligned} \tag{10}$$

where the dots refer to the terms of the expression, which do not contain pseudo accelerations and have therefore no relevance later. To make the expressions to be more compact, we use the angular frequency

$$\omega_\mathrm{h} = \sqrt{\frac{g}{h}}\,, \tag{11}$$

furthermore, we introduce the dimensionless skater position, the dimensionless skater height and the dimensionless velocity as:

$$B = \frac{b\tan\kappa}{l}\,, \quad H = \frac{h\tan\kappa}{l}\,, \quad V(t) = \frac{v(t)}{\sqrt{gh}}\,, \tag{12}$$

respectively.

The pseudo force can be derived from the virtual power of the active forces:

$$\begin{aligned} \delta P &= \mathbf{G}\cdot\delta\mathbf{v}_{\mathrm{CoM}} + \mathbf{M}_\mathrm{h}\cdot\delta\boldsymbol{\omega}_\mathrm{s} + (-\mathbf{M}_\mathrm{h})\cdot\delta\boldsymbol{\omega}_\mathrm{b} + \mathbf{M}_{k_\mathrm{t}}\cdot\delta\boldsymbol{\omega}_\mathrm{b} \\ &= \Gamma_1\delta\sigma_1 + \Gamma_2\delta\sigma_2\,, \end{aligned} \tag{13}$$

where the velocity of the center of mass (CoM) is

$$\mathbf{v}_{\mathrm{CoM}} = \begin{bmatrix} \cdot \\ \cdot \\ -\sigma_1 h\sin\varphi \end{bmatrix}, \tag{14}$$

the angular velocities of the skater and the board are

$$\begin{aligned} \boldsymbol{\omega}_\mathrm{s} &= \begin{bmatrix} \sigma_1\cos\psi & \sigma_1\sin\psi & -\frac{v(t)}{l}\tan\kappa\sin\beta \end{bmatrix}^\mathrm{T} \quad \text{and} \\ \boldsymbol{\omega}_\mathrm{b} &= \begin{bmatrix} \sigma_2\cos\psi & \sigma_2\sin\psi & -\frac{v(t)}{l}\tan\kappa\sin\beta \end{bmatrix}^\mathrm{T}, \end{aligned} \tag{15}$$

respectively, the torque vector produced by the skater is

$$\mathbf{M}_\mathrm{h} = \begin{bmatrix} -M_\mathrm{h}\cos\psi & -M_\mathrm{h}\sin\psi & 0 \end{bmatrix}^\mathrm{T}, \tag{16}$$

the torque originated from the spring in the suspension system is

$$\mathbf{M}_{k_\mathrm{t}} = \begin{bmatrix} -k_\mathrm{t}\varphi\cos\psi & -k_\mathrm{t}\varphi\sin\psi & 0 \end{bmatrix}^\mathrm{T} \tag{17}$$

and the gravitational force is

$$\mathbf{G} = \begin{bmatrix} 0 & 0 & -mg \end{bmatrix}^\mathrm{T}. \tag{18}$$

Finally, the governing equations of the system can be given as

$$\begin{aligned} \frac{\dot{\sigma}(t)}{\omega_\mathrm{h}} &= \frac{K_\mathrm{t}}{K-1}\left((2K-1)\left(D\sigma(t-\tau) + P\omega_\mathrm{h}\varphi(t-\tau)\right)\right. \\ &\quad -K\omega_\mathrm{h}(\beta(t)-\varphi(t))) - B\dot{\beta}(t)(A\omega_\mathrm{h}t + V_0)\cos(\beta(t))\cos(\varphi(t)) \\ &\quad + H\omega_\mathrm{h}(A\omega_\mathrm{h}t + V_0)^2\sin(\beta(t))\cos(\varphi(t)) \\ &\quad \times (H\sin(\beta(t))\sin(\varphi(t)) - 1) \\ &\quad + \omega_\mathrm{h}\sin(\varphi(t)) - B\sin(\beta(t))\cos(\varphi(t))A\omega_\mathrm{h}\,, \\ \dot{\varphi}(t) &= \sigma(t)\,, \\ \frac{\dot{x}(t)}{l} &= H\omega_\mathrm{h}\cot\kappa(A\omega_\mathrm{h}t + V_0)(\cos(\psi(t) + B\sin(\beta(t))\sin(\psi(t))))\,, \\ \frac{\dot{y}(t)}{l} &= H\omega_\mathrm{h}\cot\kappa(A\omega_\mathrm{h}t + V_0)(\sin(\psi(t)) - B\sin(\beta(t))\cos(\psi(t)))\,, \\ \dot{\psi}(t) &= -H\omega_\mathrm{h}(A\omega_\mathrm{h}t + V_0)\sin(\beta(t))\,, \\ \beta(t) &= \frac{K}{(2K-1)}\varphi(t) + P\varphi(t-\tau) + \frac{D}{\omega_\mathrm{h}}\sigma(t-\tau)\,, \end{aligned} \tag{19}$$

where the new parameters related to the human control and the speed are the dimensionless proportional and differential gains, the dimensionless suspension and muscle stiffnesses, the dimensionless initial speed and the dimensionless longitudinal acceleration:

$$P = \frac{p}{k_\mathrm{t}}\,,\ D = \frac{d}{k_\mathrm{t}}\sqrt{\frac{g}{h}}\,,\ K_\mathrm{t} = \frac{k_\mathrm{t}}{mgh}\,,\ K = \frac{k}{k+k_\mathrm{t}}\,,$$
$$V_0 = \frac{v_0}{\sqrt{gh}}\,,\ A = \frac{a}{g}\,, \tag{20}$$

respectively. Here we used the notation $\sigma = \sigma_1$ and used $\dot\beta$ for σ_2 for the sake of brevity.

Note that, the governing equations of the position (x, y) and the direction (ψ) of the board are not important from stability point of view, since only the body angle of the skater is controlled. Moreover, an algebraic equation arises for the deflection angle of the board (β) due to its neglected mass moment of inertia resulting in a second order explicit time-dependent neutrally delayed system after the substitution of β.

3 Linear stability analysis

The linearized equation of motion of the skater balancing around the trivial solution (rectilinear motion) with respect to small perturbations in σ and φ is

$$\dot{\mathbf{X}}(t) = \mathbf{A}(t)\mathbf{X}(t) + \mathbf{B}(t)\mathbf{X}(t-\tau) + \mathbf{C}(t)\dot{\mathbf{X}}(t-\tau)\,, \tag{21}$$

where

$$\mathbf{A}(t) = \begin{bmatrix} a_{11}(t) & a_{12}(t) \\ 1 & 0 \end{bmatrix}\,,\quad \mathbf{B}(t) = \begin{bmatrix} b_{11}(t) & b_{12}(t) \\ 0 & 0 \end{bmatrix}$$
$$\mathbf{C}(t) = \begin{bmatrix} c_{11}(t) & 0 \\ 0 & 0 \end{bmatrix} \quad \text{and} \quad \mathbf{X}(t) = \begin{bmatrix} \sigma(t) \\ \varphi(t) \end{bmatrix}\,, \tag{22}$$

with the following coefficients:

$$\begin{aligned} a_{11}(t) &= \frac{BK\omega_\mathrm{h}(A\omega_\mathrm{h}t + V_0)}{1-2K}\,, \\ a_{12}(t) &= -\frac{\omega_\mathrm{h}^2}{2K-1}\left(HK(A\omega_\mathrm{h}t+V_0)^2\right. \\ &\qquad \left. + K(K_\mathrm{t} + AB - 2) + 1\right)\,, \\ b_{11}(t) &= -\omega_\mathrm{h}\left(DH(A\omega_\mathrm{h}t+V_0)^2 + BP(A\omega_\mathrm{h}t+V_0)\right. \\ &\qquad \left. + DK_\mathrm{t} - BDA\right)\,, \\ b_{12}(t) &= -P\omega_\mathrm{h}^2\left(H(A\omega_\mathrm{h}t+V_0)^2 + K_\mathrm{t} + BA\right)\,, \\ c_{11}(t) &= -BD(A\omega_\mathrm{h}t+V_0)\,. \end{aligned} \tag{23}$$

This is an explicitly time dependent neutral delay-differential equation. In what follows, first, we are going to present a steady-state stability analysis. Then, we investigate the roots of the characteristic equation of the frozen-time system, which will be validated via numerical simulations.

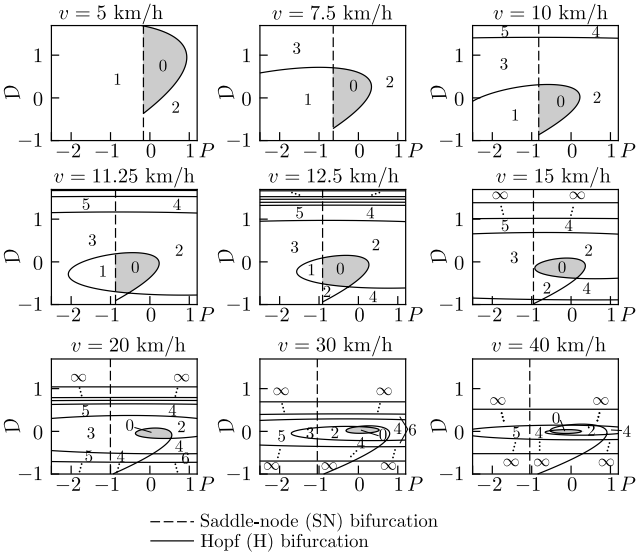

Fig. 2 Stability diagrams for different constant speeds. The intersection of the individual stable regions gives the region of frozen-time stability.

3.1 Steady state stability

The stability of the system with constant speed (i.e. $A = 0$ and $V(t) \equiv V_0$) is studied based on the characteristic function

$$\begin{aligned} D_\mathrm{c}(\lambda) = &\left(BDe^{-\lambda\tau}V_0 + 1\right)\lambda^2 + \left(e^{-\lambda\tau}D\left(K_\mathrm{t} + HV_0^2\right)V_0\right. \\ &\left. + Pe^{-\lambda\tau}B + \frac{BKV_0}{2K-1}\right)\lambda\omega_\mathrm{h} + \left(Pe^{-\lambda\tau}\left(HV_0^2 + K_\mathrm{t}\right)\right. \\ &\left. + \frac{K\left(K_\mathrm{t}-2\right) + HKV_0^2 + 1}{2K-1}\right)\omega_\mathrm{h}^2\,, \end{aligned} \tag{24}$$

where λ is the complex characteristic exponent.

In Fig. 2, typical stability charts in the parameter space of the dimensionless control gains P and D are plotted for several longitudinal speeds. Grey shading indicates the stable parameter regions and the numbers denote the number of unstable roots (with positive real parts) of the characteristic equation $D(\lambda) = 0$. The stability charts were also computed numerically using the semidiscretization method [19] with the following realistic parameters: $h = 0.85$ m, $m = 75$ kg, $g = 9.81$ m/s^2, $l = 0.3937$ m, $\kappa = 63^\mathrm{o}$, $k_\mathrm{t} = 100$ Nm, $b = 0.1$ m, $\tau = 0.3$ s. According to [20], the passive stiffness of the skater's ankle is set to 90% of the critical stiffness that would just keep the human body in the vertical position while standing on the steady ground, namely, $k = 0.9mgh = 562.85$ Nm/rad.

Since the system under analysis is governed by a neutral delay-differential equation, there are parameter regions with infinitely many unstable roots. According

to [21], this infinitely unstable region is given by

$$|D| > \frac{1}{BV_0}\,, \tag{25}$$

which occurs when the coefficient BDV_0 in the first term of Eq. (24) in absolute is larger than 1.

One can see, that the higher the speed, the smaller the stable region, and it disappears at infinitely large longitudinal speed. At low speeds, the investigated equilibrium, i.e. the rectilinear motion, can loose its stability either through a saddle-node or through a Hopf bifurcation. In case of saddle-node bifurcation, a single real characteristic exponent is crossing the imaginary axis of the complex plane, which implies a static loss of stability (simple falling). In case of Hopf bifurcation, a pair of complex conjugate characteristic exponents crosses the imaginary axis resulting in a dynamic loss of stability (oscillatory solution). At high speeds the stable region is bounded only by Hopf bifurcation.

3.2 Frozen time stability analyzes

During the frozen-time stability method, the time dependence of the coefficients are fixed over the interval $\tilde{t} \in [t_0, t_1]$ with the *frozen time* $\tilde{t}$. Since the only time dependent coefficient in (21) is the longitudinal speed $V(t) = V_0 + A\omega_\mathrm{h} t$, this approach is equivalent to replacing the time varying speed $V(t)$ by a fixed one $\tilde{V}$, called *frozen speed*. The goal is to investigate a uniform accelerating maneuver between speeds V_0 and V_1, therefore we choose $t_0 = 0$ and

$$t_1 = \frac{V_1 - V_0}{A\omega_\mathrm{h}}\,. \tag{26}$$

Thus the frozen speed is

$$\tilde{V} = A\omega_\mathrm{h}\tilde{t} + V_0\,. \tag{27}$$

The roots of the corresponding characteristic equation

$$\begin{aligned} D_\mathrm{c}(\lambda) := {} & \left(BDe^{-\lambda\tau}\tilde{V} + 1\right)\lambda^2 + \left(\frac{BK\tilde{V}}{2K-1} + BPe^{-\lambda\tau}\tilde{V}\right. \\ & \left. + De^{-\lambda\tau}\left(AB + K_\mathrm{t} + H\tilde{V}^2\right)\right)\lambda\omega_\mathrm{h} \\ & + \left(\frac{K(AB + K_\mathrm{t} - 2) + HK\tilde{V}^2 + 1}{2K-1}\right. \\ & \left. + Pe^{-\lambda\tau}\left(AB + H\tilde{V}^2 + K\right)\right)\omega_\mathrm{h}^2 = 0 \end{aligned} \tag{28}$$

are analyzed as a steady-state system for different longitudinal speeds $\tilde{V}$. Note that the characteristic equation (28) is not equivalent to equation (24), since the acceleration A does not show up in (24).

We focus on the difficulties of skateboarding at high speeds, hence v_0 is set to 5 km/h ($V_0 = 0.481$) and upper limit is the word speed record in standing position, $v_1 = 130.63$ km/h ($V_1 = 12.513$). This speed was achieved by a Swedish skater in 2016 at Les Éboulements (Quebec, Canada) with maximum 18% grade [22], so the corresponding maximal acceleration and maximal dimensionless acceleration are

$$a_\mathrm{max} = g\frac{\mathrm{grade}}{\sqrt{1 + \mathrm{grade}^2}} = 1.73787\ \mathrm{m/s^2} \tag{29}$$

and $A_\mathrm{max} = 0.177153$, respectively.

In this study, this maximal acceleration is used ($A = A_\mathrm{max}$), and those dimensionless control gain pairs ($P - D$) are declared as stable, where the characteristic equation of the corresponding frozen-time system has only roots with negative real parts for each $\tilde{V} \in [V_0, V_1]$ accordingly for each $\tilde{t} \in [t_0, t_1]$. For the computations, the longitudinal speed ($\tilde{V}$) was fixed at 100 uniformly distributed values between V_0 and V_1. Those pairs (P, D), which were stable for all the 100 cases, were indicated with dark grey shading in Fig. 3.(a). Similarly to the steady-state case, stability of the frozen-time system was determined by the semi-discretization method [19].

It is important to mention that if the initial speed is set to $v_0 = V_0 = 0$, then there is no frozen-time stable region in the parameter plane (P, D). Namely, the stable parameter region for zero speed has no intersection with the stable region for 5 km/h or larger speeds. This points out the positive effect of the speed on the stability as it was already shown by Hubbard in [1] and also highlights the differences between standing still and skateboarding. In [10], it was shown that this positive effect is valid only up to a critical speed due to the reaction delay of the skater. Therefore, riding the skateboard becomes more difficult at higher speeds.

3.3 Stability analyzes based on numerical simulations

The frozen-time method gives only an approximation of the stability of the actual explicitly time-dependent system. Therefore the stability of the system is also determined by numerical simulations. We solve the nonlinear system numerically for different control gains in the time domain $t \in [t_0, t_1]$ with the initial condition $\varphi(t) = 0$ for $t \in [-\tau, 0]$, $\dot{\varphi}(t) = \sigma(t) = 0$ for $t \in [-\tau, 0)$ and $\dot{\varphi}(0) = \sigma(0) = 0.01$. A control gain pair is declared to be finite time stable (or practically stable) if the corresponding time history of the absolute body angle is less than 10°, namely

$$|\varphi(t)| < 10^\circ = 0.087\,\mathrm{rad} \quad \text{for} \quad t \in [0, t_1]\,. \tag{30}$$

The regions associated with finite time stability are indicated by light grey shading in Fig. 3.(a).

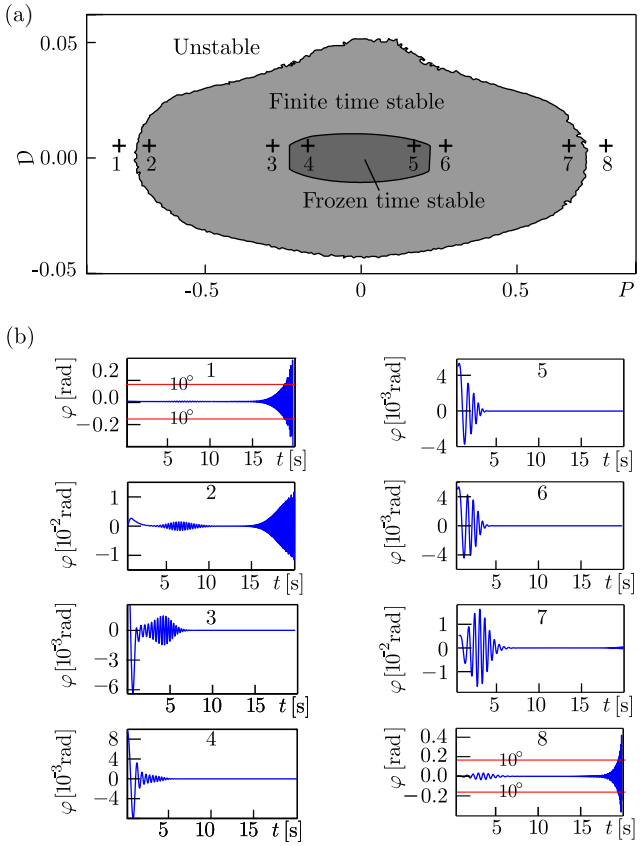

Fig. 3 (a) Stability diagram. Light grey shading indicates finite time (practical) stability, dark grey shading indicates frozen-time stability. (b) Time histories for different parameter points.

In Fig. 3.(a), one can see that the frozen-time approach gives a conservative estimate of the practical stable region obtained by numerical simulations. Cases, where oscillations increases for a short period, are declared to be unstable according to the frozen-time method, although these oscillations decays after a while and the body angle φ never exceeds the threshold 10° (see time histories 1, 2 and 3 in Fig. 3b). These solutions are therefore still finite time stable.

4 Explanations of loss of stability

There are several reasons why skateboarding is more difficult at high speeds. The steady-state analysis has shown, that the higher the speed, the smaller the stable domain, thus, proper tuning of the control gains is more crucial. The investigation of the continuously changing speed has shown unsafe speed zones, which explains the rarely and randomly occurring dynamic loss of stability.

4.1 Existence of unsafe speed zones

Time histories in Fig. 3.(b) shows some time domains where the amplitude of the body angle increases. This phenomenon is more prominent in case of time histories 6, 7, but can be observed in cases 3 and 4, too. Clearly, temporary increase of the amplitude cannot be observed in the frozen-time stable region (dark grey shading).

In Fig. 4, time histories are plotted for 3 different initial speed, where the control gains are taken from the positive quadrant of the finite time stable region (light grey shading in Fig. 3a, parameter set 3; $P = 0.6$ and $D = 0.01$). Here we assume that the skater prefers to act against the perceived direction of the body angle or the angular speed, which implies that the corresponding control gains P and D are positive. Different initial speeds corresponds to perturbations at different board speeds. The speeds where the system was perturbed are the following: panel (a) shows the original case $v_0 = 5$ km/h; panel (b) present the time history for $v_0 = 14$ km/h; and finally panel (c) shows what happens if the perturbation occurs at $v_0 = 28.6$ km/h. The unsafe speed zone can be seen clearly in panel (b). If the simulation is started with the same perturbation but at a higher speed, then the body angle exceed the threshold 10° and the skater falls, as it is shown in panel (c).

The location of these unsafe speed zones strongly depends on the control gains (as illustrated by Fig. 3.(b)), on the time delay and obviously on the slope, too. Therefore, the skater's actual conditions (e.g. how tired, how concentrated), and the slope determines the location and the size of these unstable speed zones. This explains the seemingly "unpredictable" nature of high speed loss of stability on skateboards: if the skater gets perturbation in this zone, then falling occurs otherwise the skater just run through this domain.

4.2 Effect of acceleration

The magnitude of the acceleration has a major effect on the stable regions, as it is shown by Fig. 5. In panel (a), the stable region is plotted for different board accelerations between $-a_{\max}$ and $a_{\max}$. Panel (b) was constructed such that the frozen-time stability analysis was performed 100 times for different accelerations, and the area of the stable region was determined for each acceleration. In panel (b), the relative area of the stable region is plotted versus the acceleration. Obviously, the case $a = 0$ m/s^2 has no physical meaning in this analysis, but the limit $a \to 0$ exists.

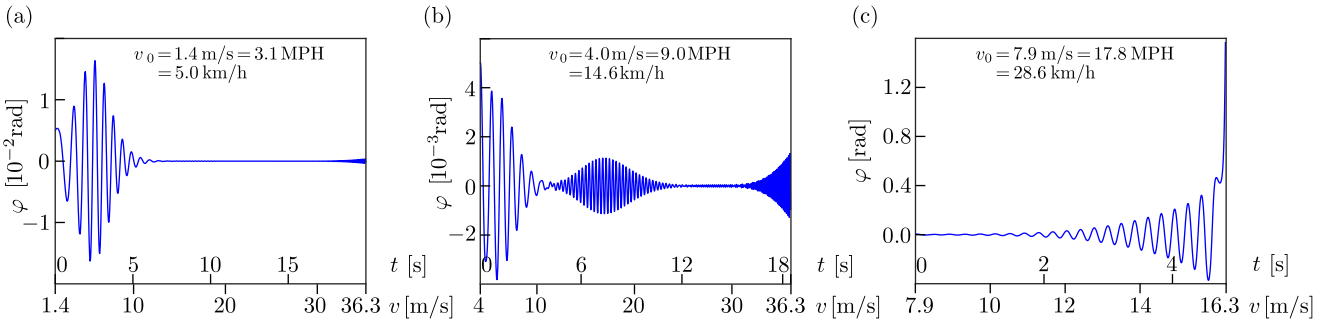

Fig. 4 Time domain simulations for different initial speeds.

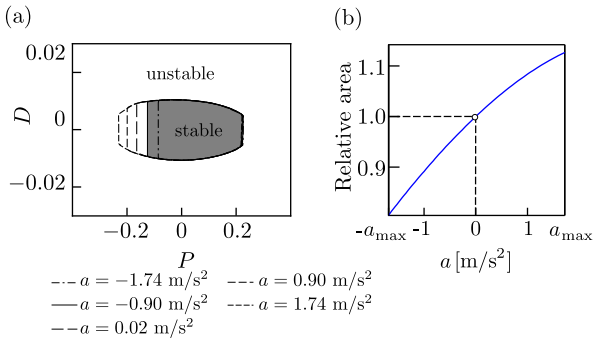

Fig. 5 (a) Stability diagrams for different board accelerations. (b) Relative area of the stable region for different accelerations.

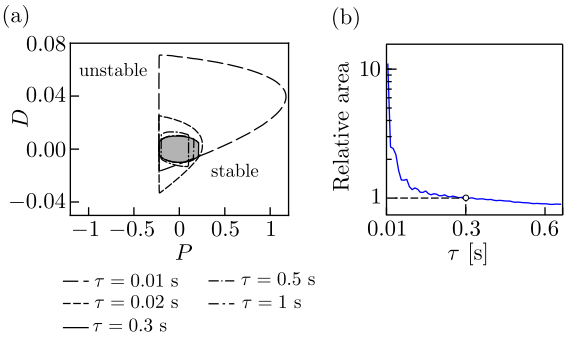

Fig. 6 (a) Stability diagrams for different reaction delays. (b) Relative area of the stable region for different reflex delays.

4.3 Effect of reaction time

The effect of the skater's reaction time is analyzed similarly to the analysis of the effect of the acceleration, namely, the frozen-time analysis is performed for 100 different reaction times ranging between 0.01 and 0.7 seconds. The results are shown in Fig. 6. In panel (a), stable regions are plotted for five different values of τ. Panel (b) shows the area of the stable region relative to the case $\tau = 0.3$ s versus the reaction time. One can see, that the higher the reaction time of the skater, the more difficult the stabilization of the skateboard. This observation is similar to the results of [10], where no acceleration was taken into account. Note that the structure of the characteristic equation (28) is similar to that of the characteristic equation of [10]. Consequently, there exists a critical reaction time delay, and the rectilinear motion cannot be stabilized for reaction delays larger than a critical delay.

5 Conclusions

A reasonably simplified model was constructed to investigate the effect of acceleration on the linear stability of human balanced skateboards. The mechanical model consist of only one lumped mass and two massless rods, while the human balancing effort is taken into account with a delayed PD controller mimicking the active torque and a spring modeling the passive stiffness of the ankle.

Based on steady-state analysis, the effect of the longitudinal speed was analyzed using the semidiscretization method. The known result of [10,23] was confirmed, namely, higher board speed results smaller stable region (hence less number of proper control gains), which exaggerates the importance of uncertainties due to the reaction delay of the skater.

The effect of acceleration was investigated using the conventional frozen-time method. Those control gain pairs were declared stable where the trivial equilibrium of corresponding neutral delay-differential equation system is stable for all investigated speeds between 5 and 130 km/h with a prescribed acceleration. The computation was performed with realistic system parameters, the maximal speed and acceleration were determined based on the actual word speed record achieved on skateboards in standing position. We showed via numerical studies that the higher the acceleration the easier the stabilization of the skateboards. Similarly the effect of the skater's reaction delay was analyzed, which confirmed that skateboarding is challenging with larger reaction delay, e.g., when the skater is tired.

The frozen-time analysis, which is based on the superposition of a series of steady-state systems, was verified via numerical simulations of the actual time-varying system. It was shown that the frozen-time method gives a conservative estimation of stability. Note that, the result of stability analysis based on numerical simulations is not unique, namely, it depends on the selected initial functions and the limit on the absolute body angle (10° in this study). The numerical simulations shown in Section 3.3 confirmed that there exist "unstable speed zones", where temporarily increasing oscillations arise. This explains the seemingly "unpredictable" loss of stability, which is often observed in high speed skateboarding. Perturbations of the skater in these (strongly parameter sensitive) unstable speed zones in most cases results in a falling.

References

1. Hubbard M (1979) Lateral dynamics and stability of the skateboard. *Journal of Applied Mechanics* 46:931–936. doi: 10.1115/1.3424680
2. Hubbard M (1980) Human control of the skateboard. *Journal of Biomechanics* 13(9):745–754. doi: 10.1016/0021-9290(80)90236-5
3. Bloch AM (2003) *Nonholonomic mechanics and control.* Springer, New York, NY, USA
4. Stepan G (2009) Delay effects in the human sensory system during balancing. *Philosophical Transactions of the Royal Society of London A: Mathematical, Physical and Engineering Sciences.* 367(1891):1195–1212
5. Insperger T, Milton J (2014) Sensory uncertainty and stick balancing at the fingertip. *Biological Cybernetics* 108(1):85–101. doi: 10.1007/s00422-013-0582-2
6. Chagdes JR, Rietdyk S, Jeffrey MH, Howard NZ, Raman A (2013) Dynamic stability of a human standing on a balance board. *Journal of Biomechanics* 46(15):2593–2602. doi: 10.1016/j.jbiomech.2013.08.012
7. Kremnev AV (2008) Dynamics and Simulation of the Simplest Model of a Skateboard. *In Proceedings of Europian Nonlinear Dynamics Conference 2008 (ENOC-2008)*, 30 June – 4 July, 2008, Saint Petersburg, Russia
8. Varszegi B, Takacs D (2016) Downhill Motion of the Skater-Skateboard System, *Periodica Polytechnica Mechanical Engineering* 60(1):58-65, doi: 10.3311/PPme.8636
9. Rosatello M, Dion Jl, Renaud F, Garibaldi L (2015) The Skateboard Speed Wobble. *In Proceedings of ASME 11th International Conference on Multibody Systems, Nonlinear Dynamics, and Control.* 2–5 August, 2015, Boston, MA, USA, doi: 10.1115/DETC2015-47326
10. Varszegi B, Takacs D, Stepan G, Hogan SJ (2016) Stabilizing skateboard speed-wobble with reflex delay, *Journal of the Royal Society Interface* 13:20160345, doi: 10.1098/rsif.2016.034
11. Wisse M, Schwab AL (2005). Skateboards, bicycles, and three-dimensional biped walking machines: velocity-dependent stability by means of lean-to-yaw coupling, *The International Journal of Robotics Research* 24(6), 417–429., doi: 10.1177/0278364905053803
12. Collins S, Ruina A, Tedrake R, Wisse M (2005) Efficient Bipedal Robots Based on Passive-Dynamic Walkers, *Science* 307(5712), 1082–1085, doi: 10.1126/science.1107799
13. Cossalter V, Lot R, Massaro M (2008) The chatter of racing motorcycles, *Vehicle System Dynamics* 46(4), 339–353, doi: 10.1080/00423110701416501
14. Weiss L, Infante E (1965) On the stability of systems defined over a finite time interval. *Proceedings of the National Academy of Sciences* 54(1):44–48
15. Moulay E, Perruquetti W (2008) Finite time stability conditions for non-autonomous continuous systems. *International Journal of Control* 81(5):797–803. doi: 10.1080/00207170701650303
16. Peterka RJ (2002) Sensorimotor integration in human postural control. *Journal of Neurophysiology* 88(3):1097–1118. doi: 10.1152/jn.00605.2001
17. Kane TR, Levinson DA (2005) *Dynamics, theory and applications.* Internet-First University Press. Ithaca, NY, USA
18. Baruh H (1999) *Analytical Dynamics.* WCB/McGraw-Hill Boston, MA, USA
19. Insperger T, Stepan G (2011) *Semi-discretization for time-delay systems – Stability and engineering applications* Springer, New York
20. Loram ID, Lakie M (2002) Direct measurement of human ankle stiffness during quiet standing: the intrinsic mechanical stiffness is insufficient for stability. *The Journal of Physiology*, 545(3):1041–1053. doi: 10.1113/jphysiol.2002.025049
21. Stepan G (1989) *Retarded dynamical systems: stability and characteristic functions* Longman Scientific, London, UK & Technical co-published with Wiley, New York, NY, USA
22. Guiness World Records [Online] Available from: http://www.guinnessworldrecords.com/ [Accessed: 18th July 2017]
23. Varszegi B, Takacs D, Stepan G (2017) Stability of Damped Skateboards Under Human Control. *Journal of Computational and Nonlinear Dynamics* 12(5):051014. doi: 10.1115/1.4036482